

# Chapter 2

## Introduction to Streaming Complex Plasmas

### A: Attraction of Like-Charged Particles

André Schella, André Melzer, Patrick Ludwig, Hauke Thomsen  
and Michael Bonitz

**Abstract** Like-charged particles usually interact via a repulsive force. However, in streaming dusty plasmas one can observe that two negatively charged dust particles may attract each other. This is explained by accumulation of positive ions below the dust particles (with respect to the streaming direction). In this chapter, we describe the dependence of this ion focus and the resulting wakes on *discharge rf-power*, *pressure* and *thermophoretic force*, as the three key parameters, that can be varied in dusty plasma experiments. Moreover, we discuss the impact of this attractive force on the collective properties of many dust particles, in particular, on the structure and on the dynamics of spherically confined clusters.

## 2.1 Introduction

Trapped charged particle systems are ideally suited model systems to study strongly coupled matter, see Refs. [1–4] and references therein. When the particle number is low, less than  $N < 1000$  say, the system is said to be finite. These systems usually require an external confinement potential to be stable. In such systems the properties

---

A. Schella (✉) · A. Melzer  
Institut für Physik, Ernst-Moritz-Arndt-Universität Greifswald, 17489 Greifswald, Germany  
e-mail: schella@physik.uni-greifswald.de

A. Melzer  
e-mail: melzer@physik.uni-greifswald.de

P. Ludwig · H. Thomsen · M. Bonitz  
Institut für Theoretische Physik und Astrophysik, Christian-Albrechts-Universität zu Kiel,  
24098 Kiel, Germany  
e-mail: ludwig@theo-physik.uni-kiel.de

H. Thomsen  
e-mail: thomsen@theo-physik.uni-kiel.de

M. Bonitz  
e-mail: bonitz@theo-physik.uni-kiel.de

may strongly vary with the particle number and depend on the symmetry (for example in the case of “magic” configurations). Similar effects are known from other fields such as nuclei or clusters. Dusty plasmas provide a unique way to analyze and control these effects. Since the dust particles in a plasma usually interact via a screened potential, where the screening parameter depends on the plasma environment, dusty plasmas bridge the gap between systems with long-range Coulomb interaction (such as trapped ions) and systems with a hard-core potential (such as granular matter, nuclear matter or neutral Fermi gases).

A common characterization of the coupling strength in dusty plasmas is the dimensionless Coulomb coupling parameter. This parameter is defined as the ratio of the typical interaction energy of neighboring particles characterized by the distance  $b_{WS}$  and the typical kinetic, thermal energy,

$$\Gamma = \frac{Q_d^2}{4\pi\epsilon_0 b_{WS}} \frac{1}{k_B T}. \quad (2.1)$$

Here,  $Q_d$  is the dust charge,  $\epsilon_0$  the vacuum dielectric permittivity,  $b_{WS}$  the Wigner-Seitz-distance and  $k_B T$  the thermal energy. When the coupling parameter exceeds unity, the system is said to be strongly coupled. With increasing  $\Gamma$ , correlation effects and long-range order develop, eventually leading to liquid and solid behavior. For an infinite three-dimensional (3D) system the phase transition from a liquid into a solid state occurs when this parameter exceeds a value of about 172...175 [5–7]. Although  $\Gamma$  is usually defined for infinite systems, the coupling parameter can still be used to characterize the coupling strength of finite 3D dust clouds [8–10]. In this case, however, the melting point may strongly vary with the particle number  $N$ , and phase transition-like behavior typically extends over a finite transition interval [11, 12].

In situations where wakefield effects are negligible, dust particles in harmonic confinement potential are found to arrange themselves to clusters with nested spherical shells [9]. Due to Yukawa-type inter-particle forces, these crystals are called “Yukawa balls” [13–16]. A very successful model to describe Yukawa balls turned out to be the one-component plasma model (Yukawa OCP) which assumes that ion-flow effects can be neglected (which is the case if the 3D dust cloud is in the plasma bulk). The Hamiltonian for the ground state (i.e. in the limit of zero kinetic energy) of an ensemble of  $N$  identical dust grains with a time independent charge<sup>1</sup>  $Q_d$  and mass  $m_d$  is then given by [17, 18]

$$E = \sum_{i=1}^N \frac{m_d}{2} \omega_0^2 r_i^2 + \sum_{i>j}^N \frac{Q_d^2}{4\pi\epsilon_0} \frac{e^{-r_{ij}/\lambda_D}}{r_{ij}}, \quad (2.2)$$

---

<sup>1</sup> While the light plasma particles have a universal charge (electrons  $q_e$ , ions  $q_i$ ), the grain charge  $Q_d$  is subject to dynamical plasma processes and may fluctuate (this will not be taken into account in this chapter). Therefore, in order to denote this difference, we use small and capital letters, respectively.

where  $r_i = |\mathbf{r}_i|$  denotes the distance of dust particle  $i$  from the trap center and  $r_{ij} = |\mathbf{r}_j - \mathbf{r}_i|$  denotes the pair distance of two particles  $i$  and  $j$ . The trap frequency enters via  $\omega_0$ . The first term in (2.2) describes the external harmonic trap which is, for simplicity, assumed to be isotropic. The second term represents the Yukawa-type interaction potential  $\Phi_Y$  of the dust particles. Shielding by the light plasma species is taken into account by the Debye length

$$\lambda_D = \left( \frac{q_e^2 \bar{n}_e}{\varepsilon_0 k_B T_e} + \frac{q_i^2 \bar{n}_i}{\varepsilon_0 k_B T_i} \right)^{-1/2}, \quad (2.3)$$

where  $q_{e,i}$ ,  $\bar{n}_{e,i}$ , and  $T_{e,i}$  denote charge, density, and temperature of electrons and ions, respectively.

Despite its simplicity, model (2.2) serves as a good starting point to analyze finite dust clouds as long as wakefield effects play a minor role [19–21]. It can be used to study the structural properties [13, 16, 22–27] as well as collective dynamical features and excitation behavior, see Refs. [28–36]. Dust clouds confined in anisotropic traps were studied as well [20, 37–40]. (For a more detailed discussion of the structural properties and the melting behavior of dust crystals, we refer the reader to the chapter “Phase Transitions in Dusty Plasmas”).

While the Yukawa OCP model (2.2) is adequate for spherical dust crystals (e.g. the plasma bulk), an ion streaming motion leads to a different type of ordering—the formation of flow-aligned strings [41–43]. This is attributed to attractive interactions [44–53] between the dust grains caused by the ion focussing below the upper grain, as described below.

In this chapter, we specially address experiments with spherically confined dust clusters with particle numbers between  $N = 2$  and  $N \approx 50$ . Of particular interest is the transition between a spherical plasma crystal with a nested shell structure (an “artificial atom”) and flow-aligned strings when the ion flow speed is increased. The goal is to gain insight into the influence of the relevant plasma parameters on the inter-particle forces, the structure of the dust clouds and their dynamics. An in-depth theoretical analysis and the computation of the ion-wake field can be found in the Chap. 3.

## 2.2 Ion Focus and Wakefield

In the very first dusty plasma experiments, particles were embedded in the sheath of the discharge. There, they formed extended crystalline structures which are known as plasma crystals [54–56]. In the horizontal plain, the particles formed a hexagonal lattice, see Refs. [54–56] and Fig. 2.1a. It was early realized that in the vertical direction, instead of a close-packed crystal structure, the particles often aligned in vertical strings, cf. Fig. 2.1b and Refs. [41, 42, 57, 58]. Such a structure was one of the first hints towards ion focusing effects. Similar observations were made for finite

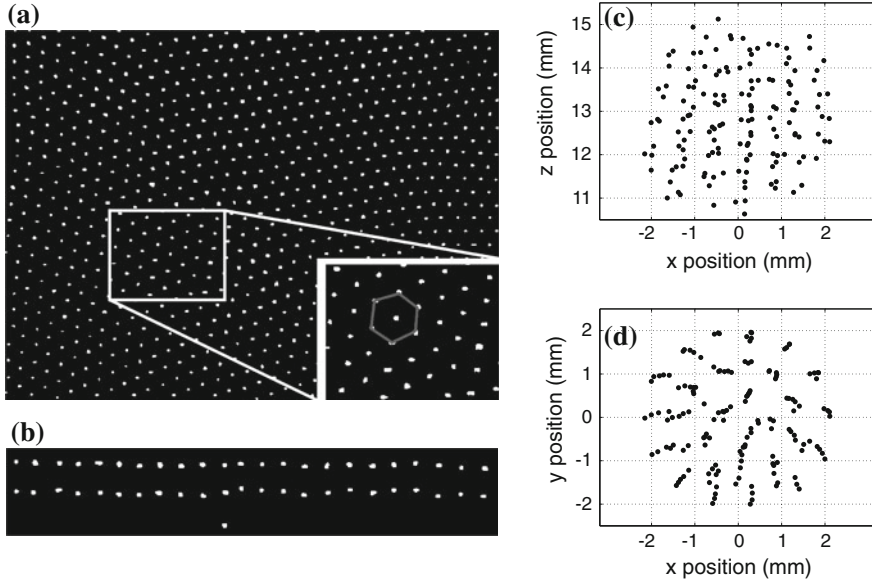


**Fig. 2.1** **a** Top view of a plasma crystal in a rf-discharge and **b** side view of the same crystal. Horizontally, the particles arrange in *hexagonal* patterns, whereas the particles are aligned *vertically*. **c** and **d** Top and side view of a finite 3D dust cloud at low pressure (Reprinted with permission from [19]. Copyright [2010], AIP Publishing LLC.). Here, the particles are aligned in vertical chains due to wakefield effects

3D dust clouds at low pressure, where it was revealed that the particles tend to form aligned particle chains in vertical direction as depicted in Fig. 2.1d [19].

### 2.2.1 Phenomenological Description of the Ion Focus

In this section, we present a phenomenological explanation for the formation of the ion wakefields and the connected attractive forces. Wakefield and ion focus are often used synonymously because they describe the same physical process where the first refers more to a wave-like picture and the second to a more particle-like picture.

A sketch of the ion focusing effect is shown in Fig. 2.2. Since the very first observations, many different approaches faced the question towards the nature of the ion wakefield attraction. In the wave-like approach, the dust particle is considered to excite ion acoustic waves that superimpose to form regions of increased positive potential. For this purpose, the dielectric response function of the ions in the vicinity of the dust particle is computed [44, 45, 59, 60]. The solution for the total (dynamically screened) potential of the dust particle is an oscillatory wake potential, the ion

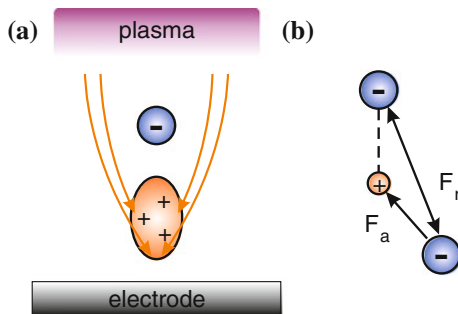


**Fig. 2.2** Sketch of the wakefield mechanism; **a** The ions are accelerated by strong electric fields in the sheath region. When streaming towards the lower electrode, they are deflected by the large grain charge that has a focusing effect giving rise to a positive space charge below the grain. **b** Reduced model of the ion focus: the space charge is replaced by a positive point charge rigidly attached to the upper dust particle. While the like-charged grains repel each other with an isotropic force  $F_r$ , grains downstream are attracted to the positive space charge by  $F_a$ . Consequently, the ion focus leads to an effective non-reciprocal grain attraction and causes a vertical grain alignment.

wakefield. The model is capable of explaining the formation of aligned particles as well as instabilities, even in the presence of collisions [48, 61–63].

The particle-based models start with a microscopic description of the ions [46, 64]. Often, the ion trajectories are solved by means of Monte-Carlo [46] or Particle-In-Cell simulations [65, 66] allowing also to study nonlinear effects [67, 68]. These models also find an enhanced ion density region, the ion focus, downstream to an upper grain leading to attractive forces on the lower particles. To explain the mechanism, we restrict ourselves to the particle-based picture. A description in form of the linear dielectric plasma response is given in the Chap. 3 by Ludwig et al.

In the sheath of the discharge, positive ions are streaming towards the electrode. When passing by a dust particle, they are attracted by the potential of the highly negatively charged dust grain, see Fig. 2.2a. The fast ions are deflected and focused below this grain creating there a positive space charge region, the ion focus [46]. A second particle placed downstream experiences the presence of this ion focus of the upper grain, see Fig. 2.2b. This leads to a superposition of the repulsive dust–dust and the attractive dust–ion interaction that can cause an alignment of the particles. In contrast, the upper particle only feels a repulsive force from the lower particle. Hence, the interaction is non-reciprocal. The non-reciprocal nature of the ion focus was proven in many experiments [19, 49–52]. Moreover, the alignment of the particles can become unstable below a critical neutral gas pressure [46]. As a result, the particles are heated by this ion-focus induced instability, that can even cause phase transitions from ordered, solid-like arrangements to liquid and gas-like situations [10, 41, 69–74].

Models suggest that there are two key parameters that strongly influence the amplitude, shape and range of the wakefield potential, namely the ion streaming velocity and the neutral gas pressure. The ion streaming velocity  $u_i$  can be described

in terms of the Mach number  $M = u_i/c_s$ , with  $c_s = (k_B T_e/m_i)^{1/2}$  being the sound (Bohm) speed [75]. From experiments deep in the sheath of the discharge, where the ion flow is supposed to be supersonic, i. e.  $M \geq 1$ , the particles inside a dust crystal are found to be on aligned particle chains [42]. However, recent investigations have demonstrated that particle chains even form at moderate ion flow velocities  $M < 1$  in 3D dust clouds [20, 76, 77], as well as in microgravity situations [78]. The second key parameter that affects the wake structure is the ion-neutral collision frequency  $\nu_i$  which is closely related to the neutral gas pressure. At low neutral gas pressure, streaming ions can move freely along their path without (or with only a few) collisions. Here, the wakefield effects are more pronounced, as confirmed by many experiments [19, 20, 42, 58, 71]. At higher damping rates, simulations suggest that the effect of the ion focus becomes weaker [63, 68].

### 2.2.2 *Biasing Wakes in the Experiment*

The experiments to study wakefield effects in dusty plasmas are manifold, see Refs. [19, 20, 42, 49, 50, 71, 77, 79–82], just to name a few. Often, one has the possibility to influence the dust–dust–interaction and the dust–confinement by varying several parameters that also affect the ion wakefield:

- By changing the neutral gas pressure  $p$ , one can change the friction force that acts on the dust particles and the ion-neutral collision rate of the streaming ions. A high pressure seems to reduce the ion focusing effect. Additionally, changing the pressure leads to changes in the local plasma environment of the dust grains.
- By adjusting the temperature of the lower electrode, one can induce an upward thermophoretic force that can be used to change the vertical position of the dust cluster in the plasma. This changes the local dust charge and the streaming velocity of the ions.
- By varying the rf-power, one changes the energy input into the discharge. This affects the densities of the plasma species and their temperatures which, in turn, has an intricate effect onto the dust charge, the confinement and the local Mach number.
- By external laser fields, one can feed energy to the dust system but leave the plasma unaffected. Moreover, driving dust clouds to fluid states by means of lasers hinders the establishment of particle alignment [10].
- By strong magnetic fields, the ions can be magnetized. This influences the wake-field attraction as well [82].

In contrast to the simulations, the Mach number is not directly controllable in the experiments. Therefore, in the experiments presented in the following, the first three parameters—(i) *neutral gas pressure*, (ii) *thermophoresis* and (iii) *rf-power*—are modified in order to study wake-affected 3D dust clusters. The parameters are closely related to Mach number  $M$ , ion-neutral collision frequency  $\nu_i$  and relative temperature  $T_e/T_i$ , which serve as an input for the simulations [63]. Thus, the great benefit

results from the possibility to compare the experimental findings with simulations presented in the Chap. 3.

## 2.3 Wakefield Effects in Dusty Plasma Experiments

In dusty plasma experiments, typically, micron-sized dust particles are immersed into a discharge plasma where they attain a high negative charge due to the steady flux of electrons and ions onto each particle's surface. Moreover, due to their high mass compared to ions and electrons, the charge to mass ratio becomes sufficiently low to trace the individual particles by means of high-speed video cameras on the kinetic level, see Refs. [2, 4, 83] and references therein.

### 2.3.1 Experimental Setup

A typical experimental setup is shown in Fig. 2.3a. Since the dust particles are all negatively charged, their mutual repulsion (even in the presence of wake effects there is repulsion between the particles that are not flow-aligned) has to be balanced by an external confinement. Trapping the dust particles inside a cubic glass box (cuvette), as shown in Fig. 2.3b, provides the great benefit to achieve harmonic confinement by a superposition of several forces acting on the individual grains [3, 9, 10, 14, 16, 19, 20, 24, 34, 39, 77, 84–87]. Radial confinement is established by the electric field, due to the dielectric glass walls. To compensate for gravity, the sheath electric field force together with a thermophoretic force from a heated lower electrode levitates the particle cloud upwards. In that manner all these forces provide a harmonic confinement where the particles form Yukawa balls, see Fig. 2.3c and Ref. [9].

Despite the harmonic confinement, the particle arrangement is influenced by ion wakefields. As described above, experiments upon Yukawa balls at high pressure reported a well established shell structure [9, 14, 16, 24]. At sufficiently low neutral gas pressure, wakefield effects due to the streaming ions become important [19, 20].

For all experiments presented in this chapter, melamine formaldehyde particles with a diameter of  $4.86\ \mu\text{m}$  (corresponding to a dust mass of  $m_d = 9.1 \cdot 10^{-14}\ \text{kg}$ ) were trapped in a cubic glass box of 2.5 cm wall length. The argon plasma is operated in a capacitively coupled radio-frequency (rf) discharge at rf-powers in the range 1–4 W and a neutral gas pressure of 4–10 Pa. Due to the low pressure used here, the establishment of wakefields can be expected in the experiments.

The dust particles are observed by imaging the scattered laser light from the grains via three orthogonal high speed cameras. These share at least one common axis and thus easily allow us to reconstruct the 3D positions. Here, particle clouds with up to hundred particles can be observed. The cameras are typically operated at frames rates up to 500 frames per second. To identify the particle positions in each image, standard

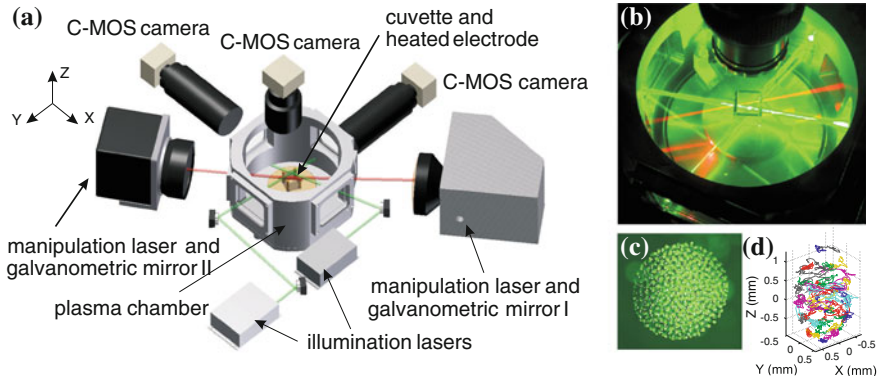


**Fig. 2.3** **a** Experimental setup used to investigate and to manipulate 3D dust clusters. **b** View into the plasma chamber; **c** Photograph of a Yukawa ball (Kädling 2008); **d** Reconstructed 3D trajectories of a laser heated cluster consisting of  $N = 48$  particles

particle identification techniques are used [88]. Afterwards, the individual particles are digitally tracked and their 3D dynamics can be retrieved, see Fig. 2.3d and Refs. [10, 16]. Hence, the full 3D particle dynamics are available at the kinetic level.

An overview about the different approaches to image and reconstruct three-dimensional dust clouds has been given in Ref. [3]. Established methods include scanning video microscopy [9, 89, 90], stereoscopic imaging [16, 91], digital in-line-holography [92], the color-gradient method [28, 93] and, more recently, the single exposure technique [94].

All dust systems in the experiments presented here were investigated with a stereoscopic imaging system pictured in Fig. 2.3a that allows us to track all particles in 3D [10, 16].

An additional surplus of our setup is the possibility to manipulate dust clusters by focused laser beams. Laser heating has become the most common method to manipulate dust ensembles [10, 95–101]. Among others, it allows us to experimentally study dust–dust-interactions [49], phase transitions [10, 97, 102] and to excite waves in dusty plasmas [103–105].

The laser beams leave the plasma itself unaffected. The dust particles respond to the momentum transferred by the radiation pressure of the beam [95, 106]. Random laser excitation of the dust particles mimics a heating process leading to increased kinetic temperatures of the dust particles [99, 100]. Thus, controlling the laser intensity allows us to change the dust temperature and, with it, vary the coupling parameter  $\Gamma \propto 1/T$  very precisely without varying other plasma properties. With the setup shown here, it is possible to cover a wide range of coupling strengths, see Fig. 2.4.



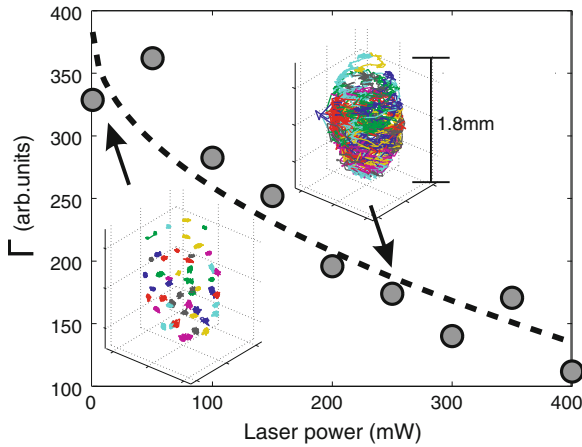


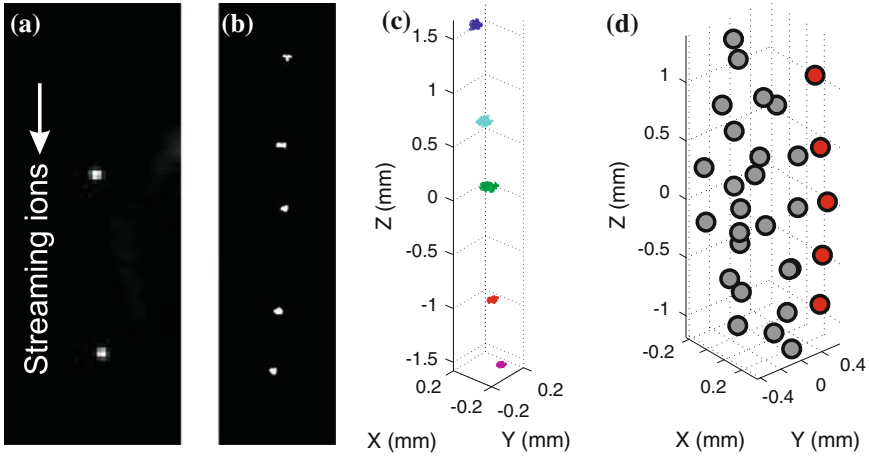
**Fig. 2.4** Coupling parameter as a function of the applied laser power (*large dots*). The inset shows typical particle trajectories for two characteristic values of  $\Gamma$ . The *dashed line* is a guide to the eye

### 2.3.2 Structure of Ion-Focus Affected 3D Dust Clusters

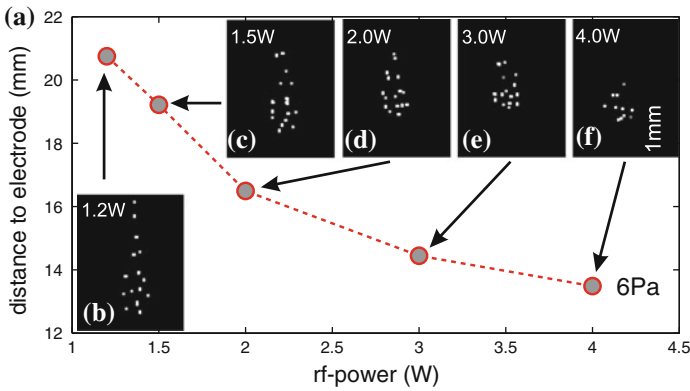
The influence of the ion focus is omnipresent in low pressure dusty plasma experiments [19, 20, 58, 71, 77, 79]. As a first insight into the complex wakefield mechanisms, we start with a brief phenomenological introduction into the structure of wake-affected 3D dust clusters. In order to study the fundamental particle–particle interaction, it is sufficient to start with a simple system of a single elongated 1D dust string.

Figure 2.5a shows a “dust molecule” formed by two particles inside the cubic glass box. The particles were confined at 6 Pa and 1.6 W rf-power. Evidently, the like-charged particles are vertically aligned. This situation is found to be very stable (see below). Further, a low rf-power is favorable to confine single dust strings [39]. Figure 2.5b shows a camera image of a vertical dust string made of five particles. The particles are aligned along the ion streaming direction. The dust chain was confined at 0.8 W rf-power at a pressure of 10 Pa. In Fig. 2.5c, the reconstructed 3D trajectories of the particles are depicted. At these experimental conditions, the particles within the cluster are nearly at rest. In general, single aligned particle chains, as shown in Fig. 2.5a–c, can even be formed for like-charged particles that obey purely repulsive interactions if the vertical confinement is much weaker than the horizontal confinement. As a representative example of a larger dust cloud, a cluster of  $N = 30$  particles with a trend to form aligned particle chains is shown in Fig. 2.5d. The highlighted particles are aligned along the ion streaming direction. This cluster structure hints towards the presence of the ion focus, because the particles in the glass box are in a nonequilibrium environment.

The competition between repulsive dust–dust interaction and attractive wakefield–dust interaction leads to a rich variety in structure and shape of the dust clouds.



**Fig. 2.5** **a** Still video image of two vertically aligned particles (“dust molecule”). **b–c** Processed video image of a single particle chain formed by  $N = 5$  dust grains and reconstructed 3D trajectories. **d** 3D positions of a  $N = 30$  cluster with trend to chain formation. A single particle chain is highlighted



**Fig. 2.6** **a** Cluster height inside the glass box as a function of the applied rf-power for a neutral gas pressure of 6 Pa. **b–f** Processed camera images of a  $N = 16$  cluster for different rf-powers. The shape changes from droplet-like to spheroidal with increasing rf-power

Therefore, it is tempting to get a deeper insight about cluster structure at different experimental conditions.

Figure 2.6a shows the distance of the center of mass of the dust cluster from the lower electrode as a function of the applied rf-power. The neutral gas pressure was kept constant at 6 Pa. At fixed thermophoretic levitation force, increasing the discharge power leads to a lowering of the cluster position inside the glass box. An increase of the discharge power causes an increased density of electrons and ions.

This, in turn, leads to a smaller Debye length and hence to a smaller sheath width and to the observed sinking of the dust clusters.

In Fig. 2.6b–f snapshots of a dust cluster formed by  $N = 16$  particles for different rf-powers are depicted. For a low discharge power of 1.1 W, Fig. 2.6b, the cluster is strongly elongated along the ion streaming direction. The uppermost particles form a single chain and the cluster looks like a droplet. By increasing the discharge power to 1.5 and 2.0 W, Fig. 2.6c–d, the inter-particle distance reduces, but the droplet-like shape remains. A further increase of the discharge power to 3.0 and 4.0 W leads to a transition from the droplet-like shape to a more spheroidal shape of the dust cloud [20], see Fig. 2.6e–f.

The ions are streaming towards the lower electrode. As discussed before, below the upper particles, the streaming ions are being focused producing a positive space charge region when the mean free path length for ion-neutral collisions becomes large [75]. This positive charge leads to an attractive force on the downstream particles and favors vertical particle alignment. The strength of the wakefield attraction depends on the Mach number  $M$  of the streaming ions. By varying the height of the cluster inside the glass box, not only this local Mach number is changed. Furthermore, the dust charge crucially depends on the local plasma parameters, which change dramatically with the vertical position of the cluster [14]. Reliable calculations of the dust charge in flowing plasmas are only starting [63, 65, 66, 107], therefore, it is still a challenging task to simulate the dust charge in a flowing environment self-consistently. From the experiment point of view, understanding the complex physical mechanisms for the cluster structure under the influence of wakefields is still an open issue. Thus, the cluster structure can serve as a hint at wakefield effects in the experiment. However, further detailed investigations of the particle dynamics are required.

### 2.3.3 Dynamics of Ion-Focus Affected 3D Dust Clusters

#### 2.3.3.1 Attraction of Two Like-Charged Particles

Two-particle dust systems are the simplest accessible system to study the interaction between like-charged particles. They have become a very attractive playground for experimentalists to study interactions and correlations [79, 108, 109] as well as wake effects [19, 49, 50, 80–82, 110].

Figure 2.7a, b shows still camera images of two dust particles inside a confining glass box are shown that form a “dust molecule” under different experimental conditions. The particles are trapped without additional thermophoretic levitation at a neutral gas pressure of 6 Pa. Thus, their equilibrium position is located where the sheath electric field force compensates gravity. In Fig. 2.7a, the particles are aligned horizontally. This is due to the high rf-power of 4.5 W which leads to a strong vertical confinement.

It is well known that reducing the discharge power weakens the vertical confinement to the dust particles in a glass box, see Refs. [20, 39] and the previous section.

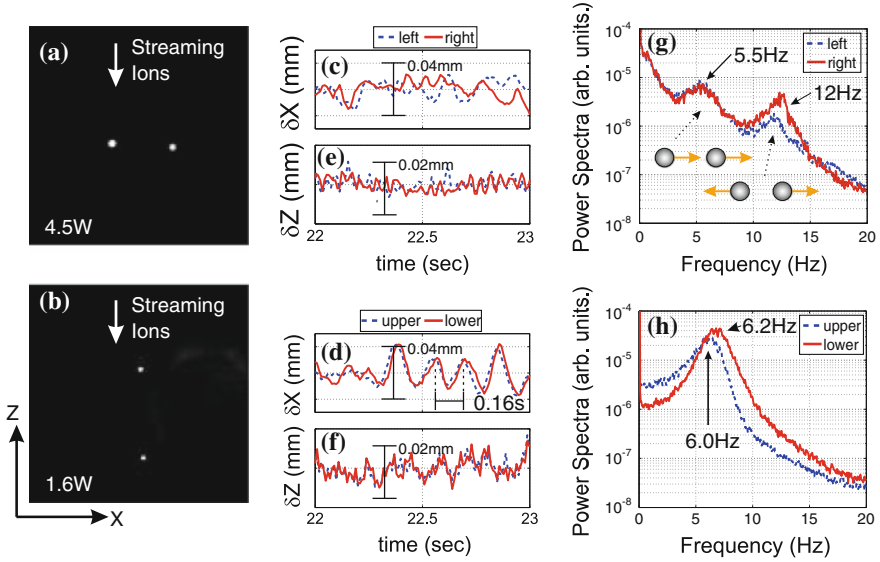


**Fig. 2.7** Still video images of two dust grains confined at 6 Pa and 4.5 W (a) and 1.6 W (b). c–f Fluctuations of the trajectories over a time span of one second. g–h Power spectra of the transverse movement of particles 1 and 2

Here, by reducing the discharge power to 1.6 W, the dust particles tend to align under each other along the ion streaming direction in Fig. 2.7b. This is due to the previously discussed ion focusing effect.

Figure 2.7c–f shows the horizontal (perpendicular to the ion flow) and vertical fluctuations of the particles’ movement over a time interval of one second. In the case of the horizontally aligned particles, Fig. 2.7c, d, the particles’ motion is not correlated, neither in horizontal nor in vertical direction. This changes drastically for the vertically aligned particles. In Fig. 2.7e, the correlated oscillatory motion is clearly visible. Moreover, the downstream particle lags behind the upper one but with a slightly larger amplitude. This means that the lower particle tries to follow the upper particle’s motion. The oscillation period can be found as  $\Delta t = 0.16$  s. Consequently, the frequency of this oscillation is  $f = 1/\Delta t = 1/0.16$  s = 6.25 Hz. Interestingly, the fluctuations along the  $z$ -direction in Fig. 2.7f do not show well established oscillations. Thus, restoring forces due to the ion focus seem to be mainly in the horizontal direction [67, 111].

Figures 2.7g, h show the power spectra of the transverse motion computed using trajectories along a time span of more than ten minutes. In the case of the horizontally aligned dust particles, both particles show two peaks in the spectra. The peak at 5.5 Hz can be identified with a center of mass oscillation in the confining potential, while the peak at 12 Hz is associated with the so called “breathing mode”-type oscillation, a radial expansion and compression of the dust system [109]. Both modes are sketched in the inset of Fig. 2.7g.

The corresponding power spectra for the particle system under the influence of an ion wakefield is shown in Fig. 2.7h. Here, only one peak in the power spectra is found. Interestingly, the peak for the upper particle is found at 6 Hz, whereas the peak of the downstream particle is found at a slightly higher frequency of 6.2 Hz. That already shows the sensitivity of dust particles to the local plasma environment. The two-particle system can serve as plasma probe, for instance to measure the sheath electric field or the dust charge [81, 112, 113].

A clear oscillatory movement and the phase delay between upper and lower particle are a direct indication of the ion focus. The downstream particle feels the attraction by this positive ion focus. In contrast, the upper particle feels the repulsive force of the downstream particle [46]. The observed aligned situation is preferred, because the lower particle follows the upper one. The source of the oscillation is not the confining potential, but the wakefield attraction. The particles experience friction due to the neutral gas. The oscillations are nonetheless persistent against this friction. Thus, to perform an oscillatory movement, the particles must gain their energy from the ion focus.

We can conclude that a two-particle systems can be used to experimentally study wake effects with high accuracy. The particles are sensitive to even little changes in the local plasma parameters. Thus, they may also serve as a valuable reference for wakefield simulations.

### 2.3.3.2 Wake-Affected Cluster Dynamics

For the sake of a broader picture, in the following, the dynamics of larger 3D dust clusters will be investigated. In order to emphasize the role of the ion wake for the cluster dynamics, experiments with a cluster consisting of  $N = 11$  particles at a pressure of 4.3 Pa are presented, see Fig. 2.8a–c. (In Fig. 2.8c, the cluster consists of  $N = 12$  particles due to an accidentally trapped additional particle, letting our conclusions unaffected). The discharge power was varied from 0.8 W to 2.4 W in order to increase the energy of the dust subsystem. The shape of the cluster changes from elongated and droplet-like, in (a), to an almost perfect sphere, in (c), which is due to the different confinement conditions, as was discussed in Sect. 2.3.2. The particles of the cluster perform oscillatory motions for all three discharge powers. At low power, Fig. 2.8a, the three uppermost particles perform a movement that resembles a wiggling fish tail.

To investigate the collective behavior in more detail, in the following, the oscillations of the three uppermost particles will be analyzed further. Figure 2.8d–f shows a time series of the transverse fluctuations (with  $\rho = (x^2 + y^2)^{1/2}$ ) of the three uppermost particles over a time span of one second. Oscillatory movement is found for all the cases. For a large inter-particle spacing and a low discharge power (0.8 W), Fig. 2.8a, the fluctuations seem to be somewhat oscillatory. At intermediate discharge powers of 1.4 W, Fig. 2.8e, the oscillations become well pronounced: The amplitude grows for particles placed downstream, and one finds a constant phase delay from top to bottom. Following the discussion in Sect. 2.3.3.1, these findings can be attributed

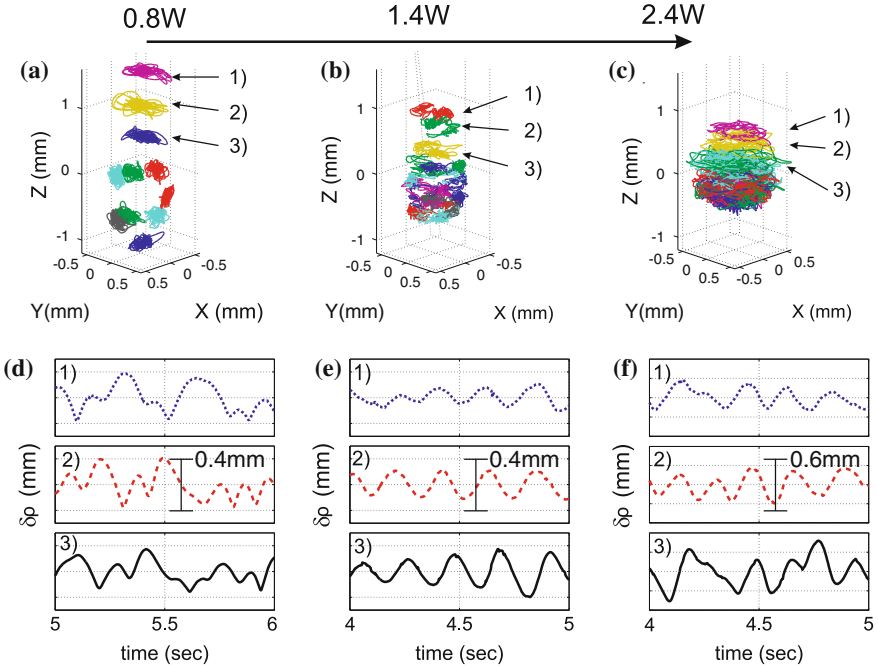


**Fig. 2.8** **a–c** Trajectories of a  $N = 11$  (12) cluster over a time span of 7s for different discharge rf-powers. **d–f** Transverse fluctuations of the three uppermost particles 1–3 corresponding to **(a)–(c)**

to the same type of oscillation as for the two-particle system. At a high discharge power of 4.0W, the cluster is clearly molten. The amplitude of the oscillations had grown further. Nonetheless, it seems that the motion of the particles 1–3 is not as correlated as in the previous case. A reason can be that at these high discharge powers the fluid-like particle motion hinders the establishment of coherent oscillations.

Finally, we draw the attention to the dynamics of entire dust clusters. An established technique to retrieve the dynamical properties of a finite system is the normal mode analysis (NMA) [18, 32, 34, 37, 114–116]. Here, it is assumed that the dust particles perform small oscillations around their equilibrium positions. This justifies an expansion of the system’s Hamiltonian, see (2.2) up to the second order, to obtain the so-called dynamical matrix

$$H = \frac{\partial^2 E}{\partial r_{\alpha,i} \partial r_{\beta,j}}, \quad (2.4)$$

with  $\alpha, \beta = x, y, z$  and  $i$  and  $j$  denoting the different particles. The solution of the corresponding eigenvalue problem of the dynamical matrix defines the  $3N$  eigenfrequencies, as well as the corresponding eigenvectors  $e_{i,l}$  of the system that define the mode pattern of eigenmode  $l$ . The mode-resolved power spectral density (PSD), i. e.

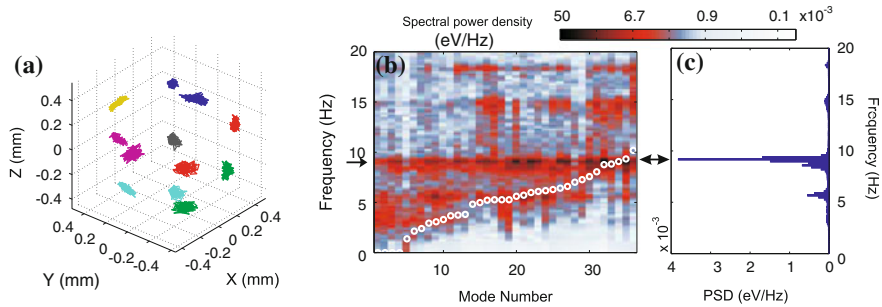


**Fig. 2.9** **a** Trajectories of a  $N = 12$  cluster over a time span of about 20 s; **b** derived power spectral density per mode and **c** corresponding PSD. Darker colors correspond to a higher energy density. The open circles correspond to calculated mode frequencies. An unstable oscillation occurs at 9.2 Hz within all modes (marked by the arrows)

the energy density per frequency interval of the  $l$ th eigenmode is calculated via [18]

$$S_l(\omega) = \frac{2}{T} \left| \int_0^T dt \left( \sum_{i=1}^N \mathbf{v}_i(t) \mathbf{e}_{i,l} \right) e^{i\omega t} \right|^2. \quad (2.5)$$

In other words, the velocity of the  $i$ -th particle  $\mathbf{v}_i(t)$  is mapped onto the  $l$ -th eigenmode and transformed into Fourier space. The PSD  $S(\omega)$ , reflecting the energy density in the frequency domain, can be obtained by summation over the mode number  $l$ , i. e.  $S(\omega) = \sum_l S_l(\omega)$ .

A NMA from the trajectories of a cluster consisting of  $N = 12$  particles was performed. The cluster was trapped at a rf-power of 3.6 W and a pressure of 5.7 Pa. From the trajectories, Fig. 2.9, it can be seen that the cluster is spherical in shape and that the cluster particles only perform small oscillations around their equilibrium positions. Thus, (2.4) is a suitable approximation. In Fig. 2.9b, the mode-resolved power spectral density is shown. The mode spectra recovers the features of a weakly damped Yukawa system [32, 116], where the normal mode frequencies rise steadily with increasing mode number. Moreover, the mode spectrum has additional features: One finds a high amount of energy stored in a narrow frequency interval at approximately 9.2 Hz in most of the modes. The dominant contribution in the PSD comes exactly from this frequency domain. This phenomenon was noticed previously for flat dust clouds under the influence of an ion focus [71]. In those dust clouds, unstable oscillations at a fixed frequency were attributed to the ion-focus instability [46]. The ion-focus instability manifests itself in a distinct frequency, the oscillation is not an eigenmode of the equilibrium system of (2.2). Hence, the oscillation can be seen in almost all of the equilibrium modes. One might be up to include wakefield effects in the energy equation (2.2) to account for these modes. However, due to the asymmetry in the forces between upper and lower particle, this cannot be done in a simple manner and is a topic of ongoing investigations.

Thus, within the NMA, wakefield effects due to the streaming ions arise as a collective phenomenon that involves all dust particles of the 3D dust cluster. In larger systems, aligned particle arrangements can become unstable below a critical neutral gas pressure if the energy gain due to the ion focus is not balanced by the energy loss via friction [46, 70]. The inherently unstable situation is the cause of phase transitions in dust clouds when the neutral gas pressure is varied [58, 71].

## 2.4 Summary and Outlook

Dust clusters in streaming plasmas exhibit configurations that differ qualitatively from spherical Yukawa balls that are observed in the plasma bulk where streaming effects are negligible. In particular, the *chain formation* in low-pressure dusty plasma experiments points to the presence of an ion focus in the wakefield below the individual dust grains. This positive space charge can give rise to a net attractive force between two negatively charged dust grains. These forces cause an alignment and lead to the formation of vertical particle strings.

More precisely, when two particles are vertically aligned, the lower particle directly follows the upper particle's motion, via the attractive ion-mediated force. In contrast, the oscillatory motion of two horizontally aligned particles is essentially uncorrelated. By varying the parameters of the discharge, namely rf-power and pressure, the structure of the dust cluster changes dramatically from a spheroidal to chain-like form with (unstable) particle oscillations. This complexity reflects the complex nature of the dust-plasma interaction in a flowing environment.

Due to its non-reciprocal nature, the ion wake force is capable of feeding energy into the dust system. Below a critical neutral gas pressure, the energy gain due to the streaming ions cannot be dissipated by friction and, thus, leads to the ion-focus instability. This instability manifests itself in unstable oscillations at a certain frequency in the power spectral density. To conclude, the actual particle interaction force depends on the pressure, the rf-power and on the thermophoresis which controls the vertical position of the cluster and, therefore, on the local Mach number. Thus, the experimental findings are a challenging input for theory and simulations.

**Acknowledgments** We would like to thank M. Mulsow for help with the data processing. We acknowledge financial support of the Deutsche Forschungsgemeinschaft via SFB-TR24, projects A3, A7 and A9.

## References

1. G.E. Morfill, A.V. Ivlev, Complex plasmas: an interdisciplinary research field. *Rev. Mod. Phys.* **81**, 1353 (2009)
2. M. Bonitz, C. Henning, D. Block, Complex plasmas: a laboratory for strong correlations. *Rep. Prog. Phys.* **73**, 066501 (2010)



3. M. Bonitz, N. Horing, P. Ludwig (eds.), in *Introduction to Complex Plasmas*. Springer Series on Atomic, Optical, and Plasma Physics (Springer, Heidelberg, 2010)
4. A. Ivlev, H. Löwen, G. Morfill, C.P. Royall, in *Complex Plasmas and Colloidal Dispersions: Particle-Resolved Studies of Classical Liquids and Solids*. Series in Soft Condensed Matter, vol 5 (World Scientific Pub Co, Singapore, 2012)
5. S. Ichimaru, Strongly coupled plasmas: high density classical plasmas and degenerate electron liquids. *Rev. Mod. Phys.* **54**, 1017 (1982)
6. H. Ikezi, Coulomb solid of small particles in plasmas. *Phys. Fluids* **29**, 1764 (1986)
7. S. Hamaguchi, R. Farouki, D.H.E. Dubin, Triple point of Yukawa systems. *Phys. Rev. E* **56**, 4671 (1997)
8. J. Schiffer, Melting of crystalline confined plasmas. *Phys. Rev. Lett.* **88**, 205003 (2002)
9. O. Arp, D. Block, A. Piel, A. Melzer, Dust Coulomb balls: three-dimensional plasma crystals. *Phys. Rev. Lett.* **93**, 165004 (2004)
10. A. Schella, T. Miksch, A. Melzer, J. Schablinski, D. Block, A. Piel, H. Thomsen, P. Ludwig, M. Bonitz, Melting scenarios for 3D dusty plasma clusters. *Phys. Rev. E* **84**, 056402 (2011)
11. A. Filinov, M. Bonitz, Y. Lozovik, Wigner crystallization in mesoscopic 2D electron systems. *Phys. Rev. Lett.* **86**, 3851 (2001)
12. J. Böning, A. Filinov, P. Ludwig, H. Baumgartner, M. Bonitz, Y.E. Lozovik, Melting of trapped few-particle systems. *Phys. Rev. Lett.* **100**, 113401 (2008)
13. M. Bonitz, D. Block, O. Arp, V. Golubnychiy, H. Baumgartner, P. Ludwig, A. Piel, A. Filinov, Structural properties of screened Coulomb balls. *Phys. Rev. Lett.* **96**, 075001 (2006)
14. O. Arp, D. Block, M. Klindworth, A. Piel, Confinement of Coulomb balls. *Phys. Plasmas* **12**, 122102 (2005)
15. H. Baumgartner, H. Kählert, V. Golobnychiy, C. Henning, S. Käding, A. Melzer, M. Bonitz, Shell structure of Yukawa balls. *Contrib. Plasma Phys.* **47**, 281 (2007)
16. S. Käding, D. Block, A. Melzer, A. Piel, H. Kählert, P. Ludwig, M. Bonitz, Shell transitions between metastable states of Yukawa balls. *Phys. Plasmas* **15**, 073710 (2008)
17. V.M. Bedanov, F.M. Peeters, Ordering and phase transitions of charged particles in a classical finite two-dimensional system. *Phys. Rev. B* **49**, 2667 (1994)
18. A. Melzer, M. Klindworth, A. Piel, Normal modes of 2D finite Coulomb clusters in complex plasmas. *Phys. Rev. Lett.* **87**, 115002 (2001)
19. M. Kroll, J. Schablinski, D. Block, A. Piel, On the influence of wakefields on three-dimensional particle arrangements. *Phys. Plasmas* **17**, 013702 (2010)
20. C. Killer, A. Schella, T. Miksch, A. Melzer, Vertically elongated 3D Yukawa clusters in dusty plasmas. *Phys. Rev. B* **84**, 054104 (2011)
21. A. Schella, M. Mulsow, A. Melzer, J. Schablinski, D. Block, From transport to disorder: thermodynamic properties of finite dust clouds. *Phys. Rev. E* **87**, 063102 (2013)
22. H. Totsuji, T. Kishimoto, C. Totsuji, K. Tsuruta, Competition between two forms of ordering in finite Coulomb clusters. *Phys. Rev. Lett.* **88**, 125002 (2002)
23. P. Ludwig, S. Kosse, M. Bonitz, Structure of spherical three-dimensional Coulomb crystals. *Phys. Rev. E* **71**, 046403 (2005)
24. D. Block, M. Kroll, O. Arp, A. Piel, S. Käding, Y. Ivanov, A. Melzer, C. Henning, H. Baumgartner, P. Ludwig, M. Bonitz, Structural and dynamical properties of Yukawa balls. *Plasma Phys. Controlled Fusion* **49**, B109 (2007)
25. D. Block, S. Käding, A. Melzer, A. Piel, H. Baumgartner, M. Bonitz, Experiments on metastable states of three-dimensional trapped particle clusters. *Phys. Plasmas* **15**, 040701 (2008)
26. H. Baumgartner, V. Golobnychiy, D. Asmus, P. Ludwig, M. Bonitz, Ground states of finite spherical Yukawa crystals. *New J. Phys.* **10**, 093019 (2008)
27. P. Ludwig, H. Thomsen, K. Balzer, A. Filinov, M. Bonitz, Tuning correlations in multi-component plasmas. *Plasma Phys. Controlled Fusion* **52**, 124013 (2010)
28. T. Antonova, B.M. Annaratone, D.D. Goldbeck, V. Yaroshenko, H.M. Thomas, G.E. Morfill, Measurement of the interaction force among particles in 3D plasma clusters. *Phys. Rev. Lett.* **96**, 115001 (2006)

29. T. Antonova, B.M. Annaratone, H.M. Thomas, G.E. Morfill, Energy relaxation and vibrations in small 3D plasma clusters. *New J. Phys.* **10**, 043028 (2008)
30. S.W.S. Apolinario, F. Peeters, Melting transitions in isotropically confined three-dimensional small Coulomb clusters. *Phys. Rev. E* **76**, 031107 (2007)
31. A. Melzer, B. Buttenschön, T. Miksch, M. Passvogel, D. Block, O. Arp, A. Piel, Finite dust clusters in dusty plasmas. *Plasma Phys. Controlled Fusion* **52**, 124028 (2010)
32. C. Henning, H. Kählert, P. Ludwig, A. Melzer, M. Bonitz, Spectral properties of spherically confined dusty plasma crystals. *J. Phys. A* **42**, 214023 (2009)
33. H. Kählert, P. Ludwig, H. Baumgartner, M. Bonitz, D. Block, S. Käding, A. Melzer, A. Piel, Probability of metastable configurations in spherical three-dimensional Yukawa crystals. *Phys. Rev. E* **78**, 036408 (2008)
34. Y. Ivanov, A. Melzer, Modes of three-dimensional dust crystals in dusty plasmas. *Phys. Rev. E* **79**, 036402 (2009)
35. H. Kählert, M. Bonitz, How spherical plasma crystals form. *Phys. Rev. Lett.* **104**, 015001 (2010)
36. C. Henning, K. Fujioka, P. Ludwig, A. Piel, A. Melzer, M. Bonitz, Existence and vanishing of the breathing mode in strongly correlated finite systems. *Phys. Rev. Lett.* **101**, 045002 (2008)
37. A. Melzer, Zigzag transition of finite dust clusters. *Phys. Rev. E* **73**, 056404 (2006)
38. S.W.S. Apolinario, F. Peeters, Melting of anisotropically confined Coulomb balls. *Phys. Rev. B* **78**, 024202 (2008)
39. J. Kong, T.W. Hyde, L. Matthews, K. Qiao, Z. Zhang, A. Douglass, One-dimensional vertical dust strings in a glass box. *Phys. Rev. E* **84**, 016411 (2011)
40. A. Radzvilavičius, O. Rancova, E. Anisimovas, Dimensional transitions in small Yukawa clusters. *Phys. Rev. E* **86**, 016404 (2012)
41. A. Melzer, V.A. Schweigert, I.V. Schweigert, A. Homann, S. Peters, A. Piel, Structure and stability of the plasma crystal. *Phys. Rev. E* **54**, 46 (1996)
42. K. Takahashi, T. Oishi, K. Shimomai, Y. Hayashi, S. Nishino, Analyses of attractive forces between particles in Coulomb crystal of dusty plasmas by optical manipulations. *Phys. Rev. E* **58**, 7805 (1998)
43. J. Hammerberg, D. Lemons, M. Murillo, D. Winske, Molecular dynamics simulations of plasma crystal formation including wake effects. *IEEE Trans. Plasma Sci.* **29**(2), 247 (2001)
44. S.V. Vladimirov, M. Nambu, Attraction of charged particulates in plasmas with finite flows. *Phys. Rev. E* **52**, R2172 (1995)
45. F. Melandsø, J. Goree, Polarized supersonic plasma flow simulation for charged bodies such as dust particles and spacecraft. *Phys. Rev. E* **52**, 5312 (1995)
46. V.A. Schweigert, I.V. Schweigert, A. Melzer, A. Homann, A. Piel, Alignment and instability of 'dust' crystals in plasmas. *Phys. Rev. E* **54**, 4155 (1996)
47. O. Ishihara, S.V. Vladimirov, Wake potential of a dust grain in a plasma with ion flow. *Phys. Plasmas* **4**(1), 69 (1997)
48. D. Winske, W. Daughton, D.S. Lemons, M.S. Murillo, Ion kinetic effects on the wake potential behind a dust grain in a flowing plasma. *Phys. Plasmas* **7**(6), 2320 (2000)
49. A. Melzer, V. Schweigert, A. Piel, Transition from attractive to repulsive forces in dust molecules in a plasma sheath. *Phys. Rev. Lett.* **83**, 3194 (1999)
50. G.A. Hebner, M.E. Riley, Measurement of attractive interactions produced by the ion wakefield in dusty plasmas using a constrained collision geometry. *Phys. Rev. E* **68**, 046401 (2003)
51. A.A. Samarian, S.V. Vladimirov, Dust particle alignments in a plasma sheath. *Contrib. Plasma Phys.* **49**(4-5), 260 (2009)
52. A. Melzer, Laser-experiments on particle interactions in strongly coupled dusty plasma crystals. *Phys. Scr.* **T89**, 33 (2001)
53. M. Kroll, J. Schablinski, D. Block, A. Piel, On the influence of wakefields on three-dimensional particle arrangements. *Phys. Plasmas* **17**(1), 013702 (2010)
54. J.H. Chu, I. Lin, Direct observation of Coulomb crystals and liquids in strongly coupled rf dusty plasmas. *Phys. Rev. Lett.* **72**, 4009 (1994)

55. Y. Hayashi, K. Tachibana, Observation of Coulomb crystal formation from carbon particles grown in a methane plasma. *Jpn. J. Appl. Phys.* **33**, L804 (1994)
56. H. Thomas, G.E. Morfill, V. Demmel, J. Goree, B. Feuerbacher, D. Möhlmann, Plasma crystal—Coulomb crystallization in a dusty plasma. *Phys. Rev. Lett.* **73**, 652 (1994)
57. T. Trottenberg, A. Melzer, A. Piel, Measurement of the electric charge on particulates forming Coulomb crystals in the sheath of an rf plasma. *Plasma Sources Sci. Technol.* **4**, 450 (1995)
58. A. Melzer, A. Homann, A. Piel, Experimental investigation of the melting transition of the plasma crystal. *Phys. Rev. E* **53**, 2757 (1996)
59. M. Nambu, S.V. Vladimirov, P.K. Shukla, Attractive forces between charged particulates in plasmas. *Phys. Lett. A* **203**, 40 (1995)
60. F. Melandsø, Heating and phase transitions of dust plasma crystals in a flowing plasma. *Phys. Rev. E* **55**, 7495 (1997)
61. M. Lampe, G. Joyce, G. Ganguli, Interactions between dust grains in a dusty plasma. *Phys. Plasmas* **7**, 3851 (2000)
62. M. Lampe, G. Joyce, G. Ganguli, Structure and dynamics of dust in streaming plasma: dust molecules, strings, and crystals. *IEEE Trans. Plasma Sci.* **33**, 57 (2005)
63. P. Ludwig, W.J. Miloch, H. Kählert, M. Bonitz, On the wake structure in streaming complex plasmas. *New J. Phys.* **14**(5), 053016 (2012)
64. A. Piel, Alignment of dust particles by ion drag forces in subsonic flows. *Phys. Plasmas* **18**, 073704 (2011)
65. W.J. Miloch, M. Kroll, D. Block, Charging and dynamics of a dust grain in the wake of another grain in flowing plasmas. *Phys. Plasmas* **17**, 103703 (2010)
66. V.R. Ikkurthi, K. Matyash, A. Melzer, R. Schneider, Computation of charge and ion drag force on multiple static spherical dust grains immersed in rf discharges. *Phys. Plasmas* **17**, 103712 (2010)
67. I.H. Hutchinson, Forces on a small grain in the nonlinear plasmawake of another. *Phys. Rev. Lett.* **107**, 095001 (2011)
68. I.H. Hutchinson, C.B. Haakonsen, Collisional effects on nonlinear ion drag force for small grains. *Phys. Plasmas* **20**, 083701 (2013)
69. H. Thomas, G.E. Morfill, Melting dynamics of a plasma crystal. *Nature* **379**, 806 (1996)
70. V.A. Schweigert, I.V. Schweigert, A. Melzer, A. Homann, A. Piel, Plasma crystal melting: a nonequilibrium phase transition. *Phys. Rev. Lett.* **80**, 5345 (1998)
71. Y. Ivanov, A. Melzer, Melting dynamics of finite clusters in dusty plasmas. *Phys. Plasmas* **12**, 072110 (2005)
72. S.K. Zhdanov, A.V. Ivlev, G.E. Morfill, Mode-coupling instability of two-dimensional plasma crystals. *Phys. Plasmas* **16**, 083706 (2009)
73. L. Couëdel, V. Nosenko, A.V. Ivlev, S.K. Zhdanov, H.M. Thomas, G.E. Morfill, Direct observation of mode-coupling instability in two-dimensional plasma crystals. *Phys. Rev. Lett.* **104**, 195001 (2010)
74. T.B. Röcker, A.V. Ivlev, R. Kompaneets, G.E. Morfill, Mode coupling in two-dimensional plasma crystals: role of the wake model. *Phys. Plasmas* **19**, 033708 (2012)
75. A. Piel, *Plasma Physics: An Introduction to Laboratory, Space, and Fusion Plasmas* (Springer, Heidelberg, 2010)
76. P. Ludwig, H. Kählert, M. Bonitz, Ion-streaming induced order transition in three-dimensional dust clusters. *Plasma Phys. Controlled Fusion* **54**, 045011 (2012)
77. L. Wörner, C. Räth, V. Nosenko, S.K. Zhdanov, H.M. Thomas, G.E. Morfill, J. Schablinski, D. Block, String structures in driven 3D complex-plasma clusters. *Europhys. Lett.* **100**(3), 35001 (2012)
78. O. Arp, J. Goree, A. Piel, Particle chains in a dilute dusty plasma with subsonic ion flow. *Phys. Rev. E* **85**, 046409 (2012)
79. V. Steinberg, R. Sütterlin, A.V. Ivlev, G. Morfill, Vertical pairing of identical particles suspended in the plasma sheath. *Phys. Rev. Lett.* **86**, 4540 (2001)
80. A.A. Samarian, S.V. Vladimirov, B. James, Wake-induced symmetry-breaking of dust particle arrangements in a complex plasma. *JETP Lett.* **82**, 858 (2005)

81. J. Carstensen, F. Greiner, D. Block, J. Schablinski, W.J. Miloch, A. Piel, Charging and coupling of a vertically aligned particle pair in the plasma sheath. *Phys. Plasmas* **19**, 033702 (2012)
82. J. Carstensen, F. Greiner, A. Piel, Ion-wake-mediated particle interaction in a magnetized-plasma flow. *Phys. Rev. Lett.* **109**, 135001 (2012)
83. G.E. Morfill, A.V. Ivlev, H.M. Thomas, Complex (dusty) plasmas kinetic studies of strong coupling phenomena. *Phys. Plasmas* **19**, 055402 (2012)
84. S. Käding, A. Melzer, Three-dimensional stereoscopy of Yukawa (Coulomb) balls in dusty plasmas. *Phys. Plasmas* **13**, 090701 (2006)
85. T.M. Flanagan, J. Goree, Observation of the spatial growth of self-excited dust-density waves. *Phys. Plasmas* **17**, 123702 (2010)
86. L. Wörner, V. Nosenko, A.V. Ivlev, S.K. Zhdanov, H.M. Thomas, G.E. Morfill, M. Kroll, J. Schablinski, D. Block, Effect of rotating electric field on 3D complex (dusty) plasma. *Phys. Plasmas* **18**, 063706 (2011)
87. W.D.S. Ruhunusiri, J. Goree, Synchronization mechanism and Arnold tongues for dust density waves. *Phys. Rev. E* **85**, 046401 (2012)
88. Y. Ivanov, A. Melzer, Particle positioning techniques for dusty plasma experiments. *Rev. Sci. Instrum.* **78**, 033506 (2007)
89. J. Pieper, J. Goree, R. Quinn, Three-dimensional structure in a crystallized dusty plasma. *Phys. Rev. E* **54**, 5636 (1996)
90. M. Zuzic, A.V. Ivlev, J. Goree, G.E. Morfill, H.M. Thomas, H. Rothermel, U. Konopka, R. Sütterlin, D.D. Goldbeck, Three-dimensional strongly coupled plasma crystal under gravity conditions. *Phys. Rev. Lett.* **85**, 4064 (2000)
91. J.E. Thomas, J.D. Willimas, J. Silver, Application of stereoscopic particle image velocimetry to studies of transport in a dusty (complex) plasma. *Phys. Plasmas* **11**, L37 (2004)
92. M. Kroll, D. Block, A. Piel, Digital in-line holography of dusty plasmas. *Phys. Plasmas* **15**, 063703 (2008)
93. B.M. Annaratone, T. Antonova, D.D. Goldbeck, H.M. Thomas, G.E. Morfill, Complex-plasma manipulation by radiofrequency biasing. *Plasma Phys. Controlled Fusion* **46**, B495 (2004)
94. P. Hartmann, I. Donkó, Z. Donkó, Single exposure three-dimensional imaging of dusty plasma clusters. *Rev. Sci. Instrum.* **84**, 023501 (2013)
95. M. Wolter, A. Melzer, Laser heating of particles in dusty plasmas. *Phys. Rev. E* **71**, 036414 (2005)
96. V. Nosenko, J. Goree, A. Piel, Laser method of heating monolayer dusty plasmas. *Phys. Plasmas* **13**, 032106 (2006)
97. Y. Feng, J. Goree, B. Liu, Evolution of shear-induced melting in a dusty plasma. *Phys. Rev. Lett.* **104**, 165003 (2010)
98. P. Hartmann, M.C. Sándor, A. Kovács, Z. Donkó, Static and dynamic shear viscosity of a single-layer complex plasma. *Phys. Rev. E* **84**, 016404 (2011)
99. J. Schablinski, D. Block, A. Piel, A. Melzer, H. Thomsen, H. Kählert, M. Bonitz, Laser heating of finite two-dimensional dust clusters: A. Experiments. *Phys. Plasmas* **19**, 013705 (2012)
100. H. Thomsen, H. Kählert, M. Bonitz, J. Schablinski, D. Block, A. Piel, A. Melzer, Laser heating of finite two-dimensional dust clusters: B. Simulations. *Phys. Plasmas* **19**, 023701 (2012)
101. V. Nosenko, A.V. Ivlev, G.E. Morfill, Anisotropic shear melting and recrystallization of a two-dimensional complex plasma. *Phys. Rev. E* **87**, 043115 (2013)
102. V. Nosenko, S.K. Zhdanov, A.V. Ivlev, C.A. Knapek, G.E. Morfill, 2D melting of plasma crystals: equilibrium and nonequilibrium regimes. *Phys. Rev. Lett.* **103**, 015001 (2009)
103. A. Piel, A. Homann, A. Melzer, Laser-excited waves in a plasma crystal. *Plasma Phys. Controlled Fusion* **41**, A453 (1999)
104. A. Melzer, S. Nunomura, D. Samsonov, J. Goree, Laser-excited Mach cones in a dusty plasma crystal. *Phys. Rev. E* **62**, 4162 (2000)
105. V. Nosenko, J. Goree, Z.W. Ma, A. Piel, Observation of shear-wave Mach cones in a 2D dusty-plasma crystal. *Phys. Rev. Lett.* **88**, 135001 (2002)
106. B. Liu, J. Goree, V. Nosenko, L. Boufendi, Radiation pressure and gas drag forces on a melamine-formaldehyde microsphere in a dusty plasma. *Phys. Plasmas* **10**, 9 (2003)

107. W.J. Miloch, D. Block, Dust grain charging in a wake of other grains. *Phys. Plasmas* **19**, 123703 (2012)
108. U. Konopka, G. Morfill, L. Ratke, Measurement of the interaction potential of microspheres in the sheath of a rf discharge. *Phys. Rev. Lett.* **84**, 891 (2000)
109. A.K. Mukhopadhyay, J. Goree, Two-particle distribution and correlation function for a 1D dusty plasma experiment. *Phys. Rev. Lett.* **109**, 165003 (2012)
110. G.A. Hebner, M.E. Riley, Structure of the ion wakefield in dusty plasmas. *Phys. Rev. E* **69**, 026405 (2004)
111. I.H. Hutchinson, Intergrain forces in low-Mach-number plasma wakes. *Phys. Rev. E* **85**, 066409 (2012)
112. J. Beckers, T. Ockenga, M. Wolter, W.W. Stoffels, J. van Dijk, H. Kersten, G.M.W. Kroesen, Microparticles in a collisional Rf plasma sheath under hypergravity conditions as probes for the electric field strength and the particle charge. *Phys. Rev. Lett.* **106**, 115002 (2011)
113. G. Schubert, R. Basner, H. Kersten, H. Fehske, Determination of sheath parameters by test particles upon local electrode bias and plasma switching. *Eur. Phys. J. D* **63**, 431–440 (2011)
114. V.A. Schweigert, F. Peeters, Spectral properties of classical two-dimensional clusters. *Phys. Rev. B* **51**, 7700 (1995)
115. A. Melzer, Mode spectra of thermally excited two-dimensional dust Coulomb clusters. *Phys. Rev. E* **67**, 016411 (2003)
116. A. Schella, M. Mulsow, A. Melzer, H. Kählert, D. Block, P. Ludwig, M. Bonitz, Crystal and fluid modes in three-dimensional finite dust clouds, *New J. Phys.* **15**, 113021 (2013)